

Short Communication

The Preparation and Performance of WO₃@C as a Counter Electrode Catalyst for Dye-Sensitized Solar Cell

Weizhen Cui^{1,2}, , Jing Ma¹, Kezhong Wu^{1,*}, Jing Chen¹, mingxing Wu^{1,*}

¹ Department of Chemistry and Material Science, Hebei Normal University, Shijiazhuang 050024, China

² Department of Chemistry and chemical engineering, Cangzhou normal College, Hebei Cangzhou 061001, China

*E-mail: wukzh688@163.com

Received: 5 May 2017 / Accepted: 20 September 2017 / Published: 12 November 2017

Tungsten trioxide (WO₃) loaded on activated charcoal powder (ACP) was sprayed onto ITO conductive glass for using in dye-sensitized solar cells(DSSC). The results showed that the composite electrode of WO₃@ACP had apparently catalytic activity as a counter electrode for the regeneration of the traditional iodide / triiodide (I/I³⁻) redox pair. In the dye-sensitized solar cell, the power conversion efficiency on WO₃@ACP was 5.04%, which was 3.15 times higher than 1.61% on the WO₃. The followed were the electrical properties test of cyclic voltammetry(CV), electrochemical impedance spectroscopy(EIS) and Tafel polarization curve. It was further explained that the catalytic activity of WO₃ @ ACP was obviously affected by the dispersion of WO₃ particles on activated carbon powder.

Keywords: Tungsten trioxide; activated charcoal powder; Catalyst; Counter electrode; Solar cell

1. INTRODUCTION

Dye-sensitized solar cell (DSSC) is a potential candidate to the silicon solar cell, owing to their particular advantages such as casual assembly processes, clearness, environmental friendliness, potty architectural combination, and corking plasticity[1-3]. The construction of a representative DSSC system is consisted of a counter electrode (CE), a dye-sensitized TiO₂ photoanode and an electrolyte [4-5]. The CE makes an important impact in DSSC, gathering electrons from the outward circuit and regenerating oxidoreduction couple. Generally, Pt is the usually used CE catalytic material owing to its efficiently catalytic activity, high conductivity and excellent chemical stability. While, the expensive cost and terminate reserves of Pt turn into a serious burden for the commercial application of DSSC. Thence, improve catalytic activity of CE materials and low price to substitute Pt is a huge challenge. Fortunately, a lot of Pt-free catalytic materials of polymer[6-7], carbon materials[8-9] and transition

metal compounds[10-11] have been led into DSSC to substitute the Pt CE. Besides, loading is a commonly used method to decrease the quantity of the precious metal without endowing its catalytic activity. As we all know, composite materials usually include two or more modules, such as, Pt/C[12], MoC/C[13], C/PEDOT/PSS[14], CoS/PEDOT/PSS[15], PtNP/MWCNT[16], Pt/graphene, PEDOT/graphene, CNTs/graphene, and Pt/CNT[17-19], etc. Normally, the strengths of the compound CE are as follows: firstly, a composite material is made up of the best qualities of all components by it; secondly, materials can decrease the amount of Platinum regard to the Platinum matrix composite CEs; thirdly, materials can apparently increase the catalytic activity.

Metal oxides have the strength of liable preparation and rich species in the composites. WO_2 as a counter electrode (CE) in the DSSC acquired power conversion effectiveness of 7.25% [20]. Hematite ($\alpha\text{-Fe}_2\text{O}_3$) with distinct geomorphologies such as nanofibers, nanoparticles (NP), nanorods and nanoflowers was successfully prepared by hydrothermal reactions and led into DSSC as a counter electrode (CE). The use of NP cells in a CE[21] resulted in a maximum efficiency of 4.60%. WO_3 have caused widespread concern as general materials employed in field emitters, gas sensors, electrochromic devices [22] and photooxidation of H_2O to O_2 as a photocatalyst[23]. Yet, rare report news concentrate on making use of tungsten oxides as counter electrodes in DSSC. In this work, tungsten dioxide (WO_3) that was supported on activated charcoal powder (ACP) was composed and checked as CE catalysts for using in the DSSC system.

2. EXPERIMENTAL

2.1 Main reagents

Ammonium paratungstate ($(\text{NH}_4)_{10}\text{H}_2(\text{W}_2\text{O}_7)_6$), lithium perchlorate(LiClO_4), lithium iodide(LiI), iodine(I_2), acetonitrile (Aladdin, Shanghai). Isopropano (Sinopharm, Shanghai). Titanium dioxide (TiO_2) (Degussa, Germany). N719 dye (Solaronix, Switzerland). Activated charcoal powder(ACP) (Yongda, Tianjin).

2.2 Preparation of CE catalysts

(1) WO_3 was prepared by high-temperature solid-state method. Which is, dissolving 1.2750g $(\text{NH}_4)_{10}\text{H}_2(\text{W}_2\text{O}_7)_6$ in distilled water of 5 mL. Ultrasonically distributing the solution for 1h and then diverting it to a drying oven to except the distilled water and getting the precursor of WO_3 . Afterwards, it was acquired by agglutinating the precipitate twice at 500°C for 8 h and 900°C for 9 h in air.

(2) The preparation of WO_3 @ACP was as follows. A certain number of 0.0030g ACP mixed with 0.1000g WO_3 . The solutions were dispersed for 1h to obtain the final WO_3 @ACP .

2.3 Electrode fabrication and cell fabrication

ACP, WO_3 and WO_3 @ACP CEs were prepared as follows: 125mg of ACP (or WO_3 and WO_3 @ACP) was scattered in isopropanol which had a volume of 2ml. Then, scattering the solution for

1h to acquire the atomization ointment. With a spray gun, applying the prepared ointment to the FTO glass. Afterwards, the FTO glass oiled with ACP (or WO_3 and WO_3 @ACP) membrane was sintered at $500\text{ }^\circ\text{C}$ for 0.5h in N_2 atmosphere. DSSC was made of a light-anode, an electrolyte and a counter electrode. The photoanode was used in this work with a 4 mm thick and N719 dye-sensitized TiO_2 film. The electrolyte involves $0.1\text{ M}\cdot\text{L}^{-1}$ of LiI, $0.07\text{ M}\cdot\text{L}^{-1}$ I_2 , $0.5\text{ M}\cdot\text{L}^{-1}$ 4-tert-butyl pyridine, $0.6\text{ M}\cdot\text{L}^{-1}$ 1-propyl-3-methylimidazolium iodide, and $0.1\text{ M}\cdot\text{L}^{-1}$ guanidinium thiocyanate in 3-methoxypropionitrile (MPN). A cell was assembled with two same counter electrodes to clip the electrolyte. Using a hot-melt surlyn membrane to seal the cells.

2.4 Measurements

X-ray powder diffractometer (D8 ADVANCE, Germany) to perform X-ray diffraction (XRD) gauges. Showing the characteristics of the surface morphologies of ACP, WO_3 and WO_3 @ACP by SEM, S-4800, Hitachi, Japan. Using an electrochemical workstation system (CHI 660E, Chenhua Shanghai) to show the characteristics of cyclic voltammetry (CV), electrochemical impedance spectroscopy (EIS) and Tafel-polarization experiments.

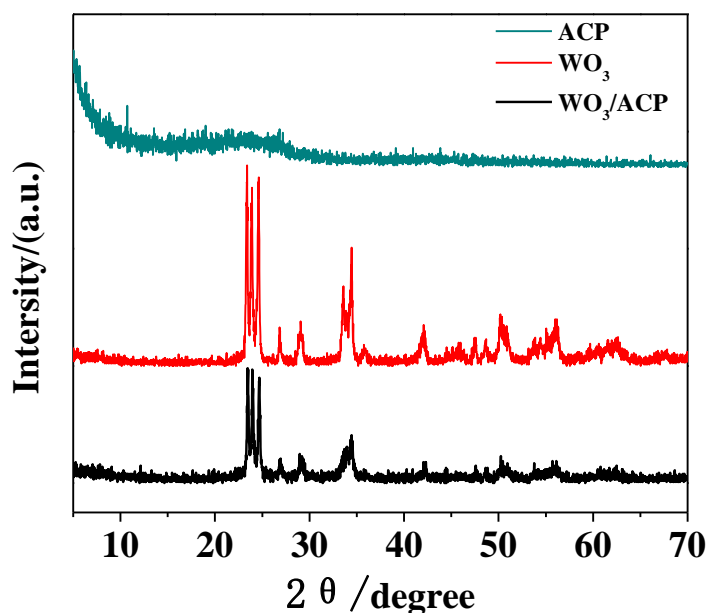


Figure 1. XRD patterns of ACP, WO_3 and WO_3 @ACP

The CV was carried out in a three-electrode system with a scanning rate of 0.02 V/s . In EIS, the gauged rate of recurrence range was from 100 mHz to 1 M Hz . The margin of the AC(alternating current) was designed at 10 mV . Measuring Tafel polarimetric measurements using electrochemical analyzers. The scan rate was 10 mV/s . The electrochemical parameter of CV, EIS and Tafel measurements, Pt was used as CE and $\text{Hg}/\text{Hg}_2\text{Cl}_2$ was stored as the reference electrode. In acetonitrile solution, the I^-/I_3^- electrolyte contains $0.1\text{ M}\cdot\text{L}^{-1}$ LiClO_4 , $1\text{ mM}\cdot\text{L}^{-1}$ I_2 , and $10\text{ mM}\cdot\text{L}^{-1}$ LiI. The electro-

PV capability of the DSSC was implemented under imitated AM 1.5 illumination ($I = 100 \text{ mWcm}^{-2}$, PEC-LO1, Yokohama, Japan) using the electrochemical workstation CHI 660E.

3. RESULTS AND DISCUSSION

3.1 Characterization of counter electrode

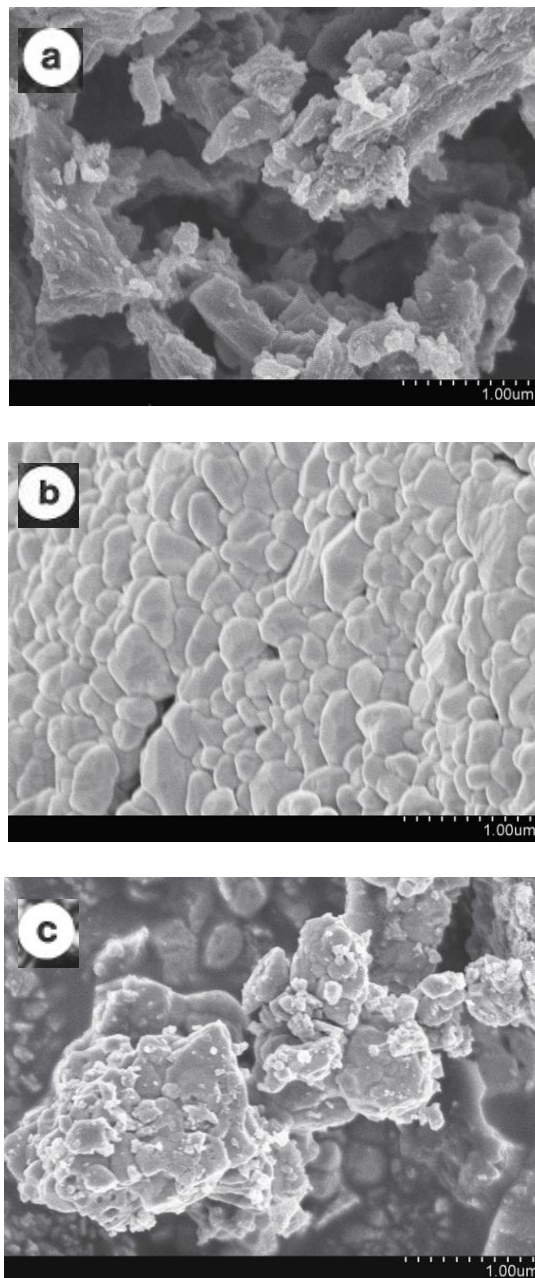


Figure 2. SEM images of the prepared (a) ACP (b) WO₃ (c) WO₃@ACP

The Fig.1 shows XRD patterns of ACP, WO₃ and WO₃@ACP. In Fig.1a indicates that WO₃ (No.32-1395, PDF-2 Database) was synthesized. The WO₃ imbedded in ACP successfully. The Fig.2 a, 2b, 2c show SEM patterns of ACP, WO₃ and WO₃@ACP. The SEM image in Fig.1c showed that

WO₃ exhibited a typical blocks and particle size was uneven, from 500nm to 2μm. Fig.2a shows that the AC is the small block. Fig.2b presented the form of blocks was bigger than ACP. Fig.2c showed that the WO₃ was loaded on ACP.

3.2 Photovoltaic performance

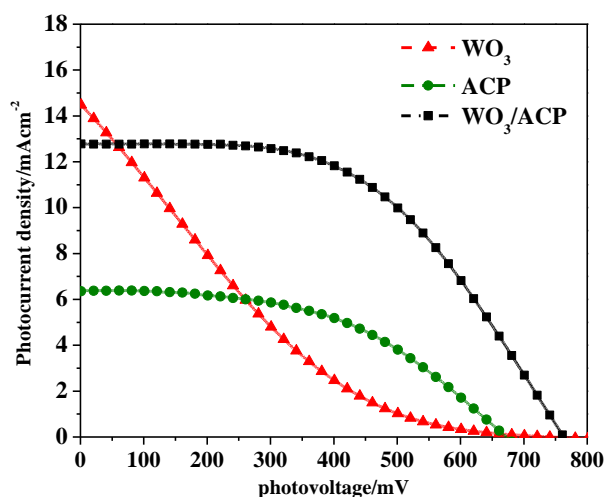


Figure 3. J–V curves of the DSSC in the I⁻/I₃⁻ electrolyte with ACP, WO₃, and WO₃@ACP

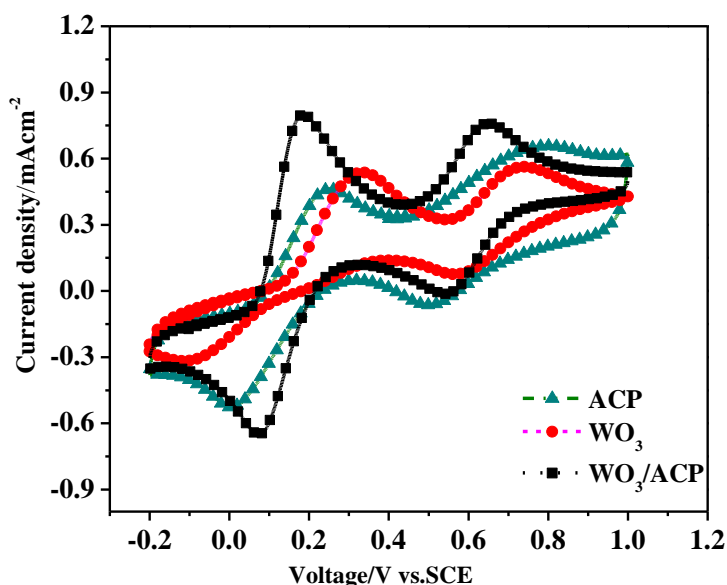


Figure 4. CV of I⁻/I₃⁻ redox couple for ACP, WO₃ and WO₃@ACP electrodes

J-V curve is the most intuitive way to reflect the performance of a battery. Therefore, in this work, we prepared WO₃, ACP, WO₃@ACP. Then, they were used as CEs in DSSC, to carry out testing. Fig4 showed the J-V curve of the DSSC using ACP, WO₃ and WO₃@ACP CEs. And the relevant PV parameters were summarized in Table 1. The WO₃@ACP showed the high catalytic

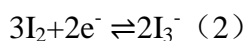
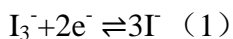
activity and the DSSC gave a PCE of 5.04%, much higher than the DSSC with the ACP (2.10%) and WO₃(1.61%). Zheng *et al.* [24] reported for the first time that WO₃ nanostructures have been used as alternative photoelectrode materials in DSSC. The commercial WO₃ nanoparticles was investigated the effect of various parameters on the cell performance. DSSC based on WO₃ nanoparticles exhibited a conversion efficiency of 0.75%, which was enhanced up to 1.46% by the surface modification. Kim *et al.* [10] reported the conversion efficiency of 1.05% for the photoelectrode based on the TiCl₄-treated WO₃ nanoparticles. In this work, the PCE was improved from 1.61% to 5.04% by tungsten dioxide (WO₃) that was supported on activated charcoal powder (ACP). The measurement results were shown that the composite materials CE could greatly reduce the cost of DSSC without sacrificing the PCE value. The WO₃@ACP fully combines the advantages and disadvantages of the ACP and WO₃.

Table 1. Photovoltaic parameters of the DSSC

Counter electrodes	V _{oc} /mV	J _{sc} /mAcm ⁻²	FF	PCE/%
ACP	673	6.38	0.49	2.10
WO ₃	745	14.50	0.15	1.61
WO ₃ @ACP	764	12.75	0.52	5.04

3.3 Electrochemical property

Fig.4 shows the CV curve of the ACP, WO₃ and WO₃@ACP electrodes in the iodide electrolyte. It can be seen from the figure 4 that the cyclic voltammetry curves have two pairs of redox peaks, corresponding to the two reactions (1) (2), the peak current density and the peak potential difference are important parameters that affect the electrocatalytic activity of the electrode[24]. The greater the peak current the smaller the peak potential difference, the better the electrocatalytic activity of the electrode, we analyze the results of the test, the current densities of the reduction peak for WO₃ was much higher than ACP. And the ΔE_p (peak-to-peak separation) of the left redox peak for WO₃@ACP (0.11V) was smaller than that of WO₃(0.45V).



CV results show that WO₃ @ ACP exhibits relatively good electrocatalytic performance during catalyzing the conversion process of I / I₃⁻. Therefore, it is a promising CE catalyst. This is also in conformity with the J-V curves results.

EIS experiments were performed with three-electrode system to investigate the electrochemical process for ACP, WO₃ and WO₃@ACP. Figure 5 shows the Nyquist diagram of the three kinds of electrode materials, whose series resistance (R_s) on the real axis and the right half arch of the load resistance (R_{ct}) are an important factor in the electrocatalytic performance of the electrode[25]. The values of the EIS electrochemical parameters were determined by fitting the EIS plots with an equivalent circuit (Fig.5). By counting the data, it can be viewed intuitively that WO₃> ACP> WO₃@ACP. The resistance of WO₃@ACP is the smallest, which indicates that it has a better electrocatalytic activity.

In order to further study the electrocatalytic activity of the three kinds of electrode materials, the Tafel curves of ACP, WO₃ and WO₃@ACP are characterized. As shown in Fig. 6.

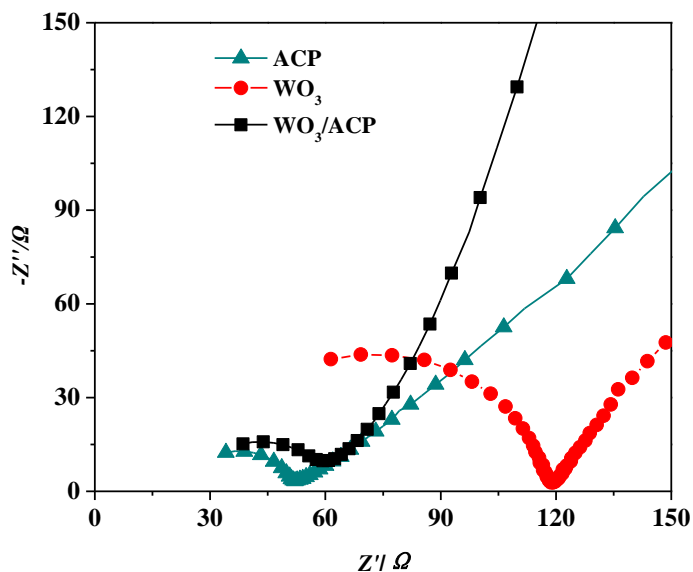


Figure 5. Nyquist plots of ACP, WO₃ and WO₃@ACP electrodes

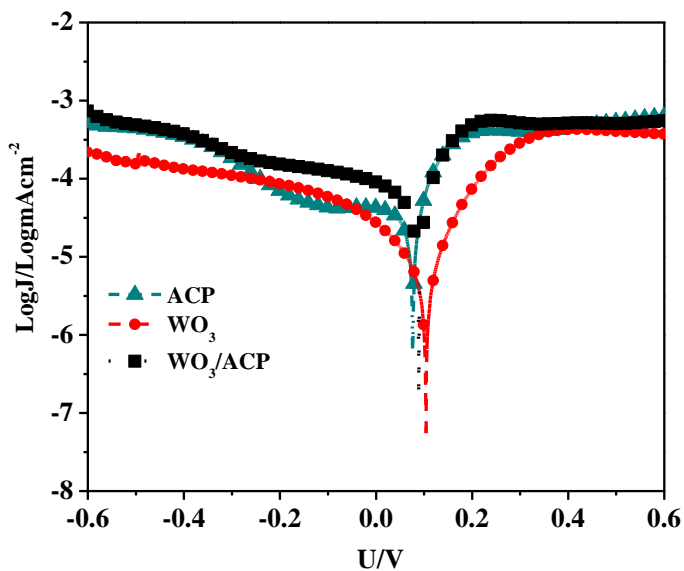


Figure 6. Tafel curves of ACP, WO₃ and WO₃@ACP electrodes

Table 2. The data of Tafel curves with ACP, WO₃ and WO₃@ACP electrodes.

electrodes	LogJ ₀ /LogmAcm ⁻²	Corrosion potential/V	LogJ _{lim} /LogmAcm ⁻²
ACP	-4.759	0.076	-3.284
WO ₃	-5.319	0.104	-3.660
WO ₃ @ACP	-4.489	0.089	-3.139

It can be seen from Fig. 6 that the three kinds of samples WO_3 , ACP and $\text{WO}_3 @ \text{ACP}$ show different polarization behavior curves, which are divided into polarized and Tafel regions according to the degree of polarization. By analyzing the Tafel curve, a series of data can be obtained of which the exchanged current density J_0 and J_{lim} have some influence factors on the electrocatalytic performance of the electrode. It can be seen that the J_{lim} of the three kinds of electrode materials is not much different, and the J_0 shows the following law. The exchanged current density (J_0) of WO_3 is much lower than $\text{WO}_3 @ \text{ACP}$, in other words, WO_3 has a lower catalytic activity than $\text{WO}_3 @ \text{ACP}$.

$$J_0 = \frac{RT}{nFR_{ct}} \quad (3)$$

Where J_0 is the exchanged current density, R is the gas constant, T is the temperature, F is Faraday's constant, n is the number of electrons involved in the reduction of triiodide at the electrode, and R_{ct} is the charge transfer resistance[26].

The J_{lim} is determined by the diffusion of the redox couple (I/I_3^-) in the electrolyte. In the diffusion zone, $\text{WO}_3 @ \text{ACP}$ shows a slightly higher J_{lim} than that of ACP and WO_3 . Base on equation (4), bigger diffusion coefficient (D) value for $\text{WO}_3 @ \text{ACP}$ was obtained. Through the data comparison of J_0 , the corrosion potential, and J_{lim} in Table 2, the parameters of the sample improved after adding activated carbon, the catalytic performance is improved.

$$D = \frac{1}{2nfc} J_{lim} \quad (4)$$

Where D is the diffusion coefficient of the triiodide in the electrolyte, l is the spacer thickness, c is the electrolyte concentration and n and f retain their established meanings[27].

By comparing the data analysis of CV, EIS and Tafel, we conclude that the addition of ACP can improve the electrocatalytic activity of WO_3 .

4. CONCLUSIONS

The WO_3 and ACP synthesized successfully were applied to the solar cell to be a counter electrode, and the photoelectric conversion efficiency of 1.61% and 2.10% was obtained respectively. In order to improve the photoelectric conversion efficiency, composite electrode materials were prepared. When WO_3 was load with ACP, the catalytic activity was improved obviously. The photoelectric conversion efficiency was 5.04% when it was used as CEs of the DSSCs. The power conversion efficiency on $\text{WO}_3 @ \text{ACP}$ is 5.04%, which is 3.15 times higher than 1.61% on the WO_3 . Approximately 80% of the battery efficiency based on Pt CE can be achieved.

Obviously, Adding the ACP can obtain the composite with the lower R_{ct} and the better catalytic activity than WO_3 . The CV, EIS and Tafel polarization curve results proved that the catalytic activity of the synthesized $\text{WO}_3 @ \text{ACP}$ was importantly affected by the dispersion of the WO_3 particles on activated charcoal powder.

ACKNOWLEDGEMENTS

This research was supported by the National Natural Science Foundation of China (No. 21473048, 21303039), the Natural Science Foundation of Hebei Province (No. B2015205163, B2016205161), and 2015 Hebei Province Undergraduate Training Programs for Innovation and Entrepreneurship. The fourteenth batch of teaching reform project of Hebei Normal University.

References

1. B. E. Hardin, H. J. Snaith, and M. D. McGehee, *Nat. Photonics*. 6(2012)162-169.
2. K. Abbas, Z. Amir, and H. Muhammad, *J. Chin. Chem. Soc.* 10(2015)915-924.
3. H.K. Zheng, H. Y. Guo, D. An, K.Z. Wu, C. J. Gao, Q. J. Han, Y. J. Zhu, Y. N. Lin, and M. X. Wu, *J. Mater. Chem. C* 4(2016)6533-6538.
4. J. Halme, P. Vaheremaa, K. Miettunen, and P. Lund, *Adv. Energy Mater.* 22(2010)E210-E234.
5. M. D. Ye, X. R. When, and M. Y. Wang, *Mater. Today*. 18(2015)155-162.
6. H. Zhou, Y. Shi, L. Wang, H. Zhang, C. Zhao, A. Hagfeldt, and T. Ma, *Chem. Commun.* 49(2013)7626-7628.
7. Y. Hou, Z. Chen, D. Wang, B. Zhang, S. Yang, H. Wang, P. Hu, H. Zhao, and H. Yang, *Small* 10(2013)484-492.
8. S. H. Chang, M.D. Lu, Y. L. Tung, and H. Y. Tuan, *ACS NANO* 79(2013)9443-9451.
9. S. Yun, L. Wang, C. Zhao, Y. Wang, and T. Ma, *Phys. Chem. Chem. Phys.* 28(2013)4286-4290.
10. S.M. Yong, T. Nikolay, B.T. Ahn, D.K. Kim, *J. Alloys Compd.* 547 (2013) 113–117.
11. B.G. Zhao, S.P. Li, M. Che, L. Zhu, *Int. J. Electrochem. Sci.* 11 (2016) 6514 – 6522.
12. S. Arman, N. M. Hoda, *Int. J. Electrochem. Sci.* 9 (2014) 2029 – 2037.
13. F. Gong, Z. Q. Li, and H. Wang, *J Mater Chem.* 22(2012)17321-17327.
14. J. H. Wu, Q. H. Li, and L. Q. Fan, *J. Power Sources*. 181(2008)172-176.
15. K. Z. Wu, J. Ma, W. Z. Cui, B. Ruan, and M. X. Wu, *J. Photochem. Photobiol. A Chem.* 340(2017) 29–34.
16. X. Zhang, X. Chen, S. Dong, Z. Liu, X. Zhou, J. Yao, S. Pang, H. Xu, Z. Zhang, and L. Li, *J. Mater. Chem. A* 1(2013)6067-6071.
17. M. X. Wu, Y. N. Lin, H. Y. Guo, and T. L. Ma, *J. Power Sources*. 263(2014)154-157.
18. G. Xin, W. Guo, and T. L. Ma, *Appl. Surf. Sci.* 256(2009)165-169.
19. K. Z. Wu, L. Chen, C. Y. Duan, J. Gao, and M. X. Wu, *Mater. Design*, 104 (2016)298–302.
20. M. X. Wu, L. Mu, Y. D. Wang, Y. N. Lin, H. Y. Guo and T. L. Ma, *J. Mater. Chem. A* 1(2014)7519-7524.
21. M. Shahpari, A. Behjat, M. Khajaminian, and N. Torabi, *Solar Energy*. 119(2015)45–53.
22. S. Adhikan, R. Swain, D. Sarkar and G. Madras, *Mol. Catal.* 432(2017)76-87.
23. D. Sudha, P. Sivakumar, *Chem. Eng. Process.* 97 (2015)112-133.
24. H.D. Zheng, Y. Tachibana, K. Kalantar-zadeh, *Langmuir*, 26 (2010) 19148–19152.
25. K. Sim, S. J. Sung, H. J. Jo, D.H. Jeon, D.H. Kim, J.K. Kang, *Int. J. Electrochem. Sci.* 8 (2013) 8272-8281
26. D.D. Song, P. Cui, X. Zhao, M.C. Li, L.H. Chu, T.Y. Wang and B. Jiang. *Nanoscale* 7(2015)5712-5718
27. Q. Zhang, Y.F. Liu, Y.D. Duan, N.Q. Fu, Q.P. Liu, Y.Y. Fang, Q.W. Sun and Y. Lin, *RSC Adv.* 4(2014) 15091-15097.